



# Evaluation of Human Body Temperature Measurements with Infrared Thermography in the Ear Region

## Kulak Bölgesinde İnfra kırmızı ışık termografi ile İnsan Vücut Sıcaklığı Ölçümlerinin Değerlendirilmesi

Devrim Önder<sup>1</sup>, Egemen Vardarlı<sup>2</sup>

<sup>1</sup>Infrared Software Research and Development Consultancy Engineering Ltd., İzmir, Türkiye

<sup>2</sup>İzmir Tinaztepe University Faculty of Medicine, Department of Neurology, İzmir, Türkiye

### ABSTRACT

**Objective:** Estimating body temperature using infrared thermography (IRT) varies in terms of measurement sites and the applied procedures. The main aim of this article is to explore the use of IRT in order to perform accurate remote human body temperature measurements using the ear region since the human ear canal is one of the most thermally closed places to external influences.

**Methods:** An observational clinical study was conducted involving 50 subjects in which forehead and tympanic body temperatures were measured by non-contact infrared thermometers as references, as well as capturing frontal and sagittal thermal images. Statistical analysis was performed on the gathered data samples and regression functions were determined for IRT measurements obtained from multiple sites against non-contact infrared thermometer references.

**Results:** We found a low agreement between forehead and tympanic non-contact infrared thermometer measurements (root-mean-square 0.79 °C). We also observed that the linear regression of tympanic non-contact infrared thermometer on sagittal IRT measurements from the right ear region provided the best results, with the clinical bias of 0.04 °C and 0.19 °C root-mean square.

**Conclusion:** We presented that real body temperature can be estimated accurately from sagittal face thermal images, especially from the rectangular region surrounding the human ear.

**Keywords:** Body temperature, fever screening, infrared thermography, regression analysis, tympanic temperature

### ÖZ

**Amaç:** İnfra kırmızı ışık termografi (IRT) kullanarak vücut sıcaklığını tahmin etmek, ölçüm yerleri ve uygulanan prosedürler açısından farklılık gösterir. Bu makalenin temel amacı, insan kulak kanalının dış etkilere termal olarak en kapalı yerlerden biri olması nedeniyle, kulak bölgesini kullanarak uzaktan insan vücut sıcaklığı ölçümleri yapmak için IRT kullanımını araştırmaktır.

**Yöntemler:** Alın ve timpanik vücut sıcaklıklarının referans olarak temassız infrared termometreler ile ölçüldüğü ve frontal ve sagittal termal görüntülerin yakalandığı 50 hasta içeren bir gözlemlsel klinik çalışma yürütülmüştür. Toplanan veri örnekleri üzerinde istatistiksel analiz yapılmış ve temassız infrared termometre referanslarına karşı birden fazla yerden elde edilen IRT ölçümleri için regresyon fonksiyonları belirlenmiştir.

**Bulgular:** Alın ve timpanik temassız infrared termometre ölçümleri arasında düşük bir uyum bulunmaktadır (karekök ortalama kare 0,79 °C). Ayrıca, sağ kulak bölgesi sagittal IRT ölçümlerinde timpanik temassız infrared termometrenin doğrusal regresyonunun 0,04 °C ve 0,19 °C karekök ortalama kare klinik sapma ile en iyi sonuçları sağladığı gözlemlenmiştir.

**Sonuç:** Gerçek vücut sıcaklığının, özellikle insan kulağını çevreleyen dikdörtgen bölgeden, sagittal yüz termal görüntülerini kullanılarak doğru bir şekilde tahmin edilebileceği sunulmuştur.

**Anahtar Kelimeler:** Vücut sıcaklığı, ateş taraması, infrared termografi, regresyon analizi, timpanik sıcaklık

**Corresponding Author/Sorumlu Yazar:** Devrim Önder, PhD  
 Infrared Software Research and Development Consultancy Engineering Ltd., İzmir, Türkiye  
 E-mail: devrim.onder@gmail.com

ORCID ID: orcid.org/0000-0003-0543-1443

Received/Geliş Tarihi: 16.06.2025 Accepted/Kabul Tarihi: 29.08.2025 Publication Date/Yayınlanma Tarihi: 31.12.2025

Cite this article as/Atıf: Önder D, Vardarlı E. Evaluation of human body temperature measurements with infrared thermography in the ear region. J Health Inst Turk. 2025;8(3):44-54



Copyright 2025 The Author. Published by Galenos Publishing House on behalf of the Health Institutes of Türkiye.  
 Licensed under a Creative Commons Attribution-ShareAlike 4.0 (CC BY-SA 4.0) International License.

## INTRODUCTION

Measurements of the vital signs provide the most important indicators of the state of the human body functions. In the field of medicine, vital signs are monitored and evaluated at the prioritization (triage), diagnosis and follow-up stages. There are four primary vital signs: pulse rate (heartbeat), respiratory rate, blood pressure and body temperature.

The main methods for human core body temperature measurement are divided into invasive and non-invasive approaches (1). The invasive approaches, mostly applied in healthcare organizations, are the most reliable ones. The invasive measurements can be performed on several sites: rectal, pulmonary artery and by swallowable temperature sensors. Non-invasive methods consist of sublingual measurement (mouth), intra-ear measurement (tympanic) and axilla (armpit) measurements.

The use of invasive and contact methods in public places is impractical and unsuitable from a hygienic point of view. Therefore, non-contact methods, which are usually based on non-contact infrared thermometers (NCITs) and infrared thermal cameras have become popular for fever screening, especially during epidemics of infectious diseases that prioritized body temperature as one of the symptoms; severe acute respiratory syndrome, H1N1, Ebola and coronavirus disease-2019 (2-5).

Infrared thermography (IRT) can be defined as the acquisition and evaluation of thermal images by using filtered lenses and infrared-sensitive bolometers. Unlike non-contact thermometers, a two-dimensional array of thermal measurements is obtained by IRT. This also creates an opportunity for the detection of certain points on the human face, allowing detailed evaluation of temperatures. An important point to note is that only outer skin temperature can be measured with IRT. If it is desired to obtain the internal body temperatures instead of just making a comparison, the skin temperature values should be transferred to references which is called conversion.

Several studies have pointed out that IRTs are not accurate for fever screening (6-9). Although recommendations for the assessment of accurate fever screening and implementation details of IRTs are presented in IEC 80601-2-59:2017 and ISO/TR 13154:2017 (10,11) standards, the processes for assessing measurement accuracy are still controversial.

There have been many studies performed on the NCIT measurement location. Bijur et al. (12) found that tympanic temperatures were more precise than temporal thermometry, with a sensitivity of 68.3% to detect a rectal temperature equivalent of 38°C. Similarly, Fong et al. (13) had an experiment

with a total of 1576 visitors to Singapore General Hospital and recorded temperatures from three different sites (i.e., temporal, forehead and tympanic) and the results demonstrated that temporal and forehead temperature readings were generally lower than those of tympanic temperature readings, and hence may not detect patients with fever. Goggins et al. (14) also concluded that the tympanic temperature was the least impacted by environmental temperature than forehead thermometers including an IRT. Mah et al. (15) compared several commercially available thermometers (including an IRT camera) with a gold standard thermometer and concluded that not all temperature monitoring techniques are equal, and suggested that tympanic thermometers are the most accurate commercially available system for the regular measurement of body temperature.

Several prior studies have investigated the relationship between oral and tympanic temperatures with core temperature and found that these sites are well-correlated candidates for core temperature (16,17). Several other studies have also proposed that the tympanic temperature is closer to the body's core temperature than forehead temperature and provides the most accurate measurements (18-21).

The inner canthi are thought to be ideal locations for non-contact temperature measurement. Inner canthi are typically the warmest regions on the face and have the highest correlation with the core body temperature due to internal carotid artery perfusion (22-24). Previous IRT studies targeting the human ear are fewer than studies focusing on frontal face thermal images. Muniz et al. (25) investigated the ear canal together with the forehead and the corner of the eye. Limpabandhu et al. (26) examined ear and temple regions together with the eyes and nose. Putrino et al. (27) found out that ears and inner canthi areas can be used as an alternative to forehead digital thermometer measurements using a thermal camera connected to a mobile device.

Several conversion approaches have been studied in past IRT research. Švantner et al. (6) examined several conversion techniques, including constant offset and normalization to approximate the reference armpit thermometer values. Limpabandhu et al. (26) used a linear regression model to successfully convert IRT values to those of an Food and Drug Administration-approved thermometer. Wang et al. (22) compared several regression models to convert IRT values to a reference oral temperature and found out that the inner canthi or facial maximum measurements provided the highest accuracy. Similarly, Sun et al. (2) converted facial IRT skin temperature to axillary temperature using linear regression.

The main aim of this study is to explore the use of infrared thermal imaging in order to perform accurate remote human

body temperature measurements from the ear region. We assumed that targeting the ear region in IRT procedure would be much more effective, since the ear canal is one of the most thermally closed places to external influences and is not affected by the use of glasses and medical masks.

## MATERIALS AND METHODS

We conducted an observational clinical research including 50 patients in İzmir Tinaztepe University Galen Medical Hospital from March to September 2021. The clinical research, which was a part of the project "Development of Artificial Intelligence-supported Software that Remotely Evaluates Human Body Temperature and Performs High Accuracy Measurements with Thermal Cameras", was approved by İzmir Tinaztepe University Health Sciences Scientific Research and Publication Ethics Committee (protocol code: TUBAYEK: 002, date: 10.03.2021). Written informed consent was obtained from all subjects.

### Environmental Conditions

The clinical study was conducted between March and September 2021. The examination room did not have air flow or any window openings. The examination room had no radiant heat sources, and the climate controller was set to keep the room temperature constant between 21-22 °C. Before each measurement, the room temperature and relative humidity measurements were recorded using a thermometer (MEDISANA HG100 Digital Thermo Hygrometer).

Based on the standard (11), the ideal environmental temperature and relative humidity intervals should be 20-24 °C and 10-50% respectively. In our study, most of the measurements were performed in the ideal room temperature interval. The room temperature mode value was 22 °C. We only had two room temperature samples (25 °C) outside the ideal interval. We also had 11 relative humidity values above the upper interval limit of 50%.

### Experimental Setup and Temperature Measurement Procedure

Volunteers for the clinical research were kept calm for 15 minutes and then taken to the imaging room. In addition, the patients did not drink any hot/cold beverages within 30 minutes and did not smoke. The people were not allowed to wear any excessive clothing or head covers (e.g., headbands and bandanas). The test area of the forehead was clean, dry and not blocked during measurements.

We used an infrared thermal camera with an uncooled microbolometer sensitive to the long-wave infrared band (T540, Teledyne FLIR LLC., USA). We set its emissivity parameter to 0.98, as described in IEC 80601-2-59:2017 standard (10).

We used Thermoval Duo Scan (Heidenheim, Germany) for forehead temperature measurement and Braun ThermoScan 6026 NCIT for tympanic temperature measurement. In their product specification documents, Thermoval declares its measurement accuracy as ( $\pm 0.2$  °C) in the 35.5-42.0 °C interval, similarly, ThermoScan declares its temperature accuracy as ( $\pm 0.2$  °C) in the temperature range 36.0-39.0 °C. These NCIT device accuracy values conform to the standard (28) about IR thermometers. There was no blackbody calibration device available.

The measurement procedure applied to all subjects was as follows:

1. At first, the subject's medical mask was removed.
2. Subject waited 30 seconds, in order to eliminate sudden temperature changes caused by the removal of the medical mask.
3. NCIT value from the middle of the forehead and tympanic region was measured.
4. The first frontal face thermal image was captured by the thermal camera.
5. A sagittal right and left head images were captured by the thermal camera.
6. The second frontal face thermal image was captured by the thermal camera.

All thermal camera images were taken from a distance of 1.0 meters against a non-reflectant wall. The time interval between consecutive thermal image captures was approximately 30 seconds. Therefore, the second frontal thermal image was captured approximately 60 seconds after the first one.

### Demographics

The subject group consisted of 21 (42%) males and 29 (58%) females. Subjects were between the ages of 21 and 88. The mean age value is 66.72 and the standard deviation (SD) value is 14.04.

### Manual Analysis of Thermal Images

All thermal images were manually analyzed using FLIR Tools software package (Teledyne FLIR LLC., USA). Measurement shapes were inserted on the thermal images and the thermal statistics were obtained. These measurement sites in frontal and sagittal (lateral) views are illustrated in (Figure 1a).

The variables (acronyms) that describe the frontal thermal image, the manual measurement area and statistics are presented in (Table 1). Similarly, the statistics for the measurement geometries presented in (Figure 1b) are obtained with corresponding variables for the sagittal thermal images (Table 2).

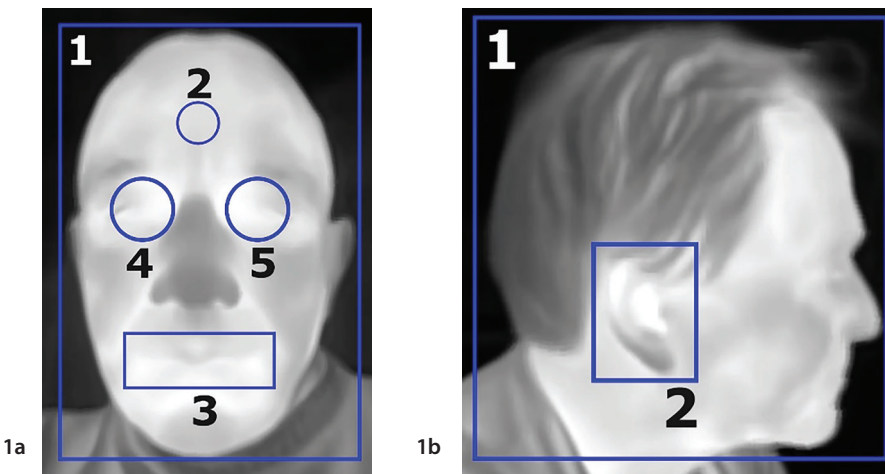


**Figure 1.** Thermal image measurement sites (a) Frontal, (1) frontal face region, (2) circular area in the forehead, (3) mouth region, (4,5) right and left canthus regions. (b) Sagittal, (1) sagittal face region, (2) ear region. Photos are of authors

**Table 1. The variables and corresponding definitions of frontal thermal image reading areas (suffix\_X represents the first and the second captured thermal image, by the number 1 or 2)**

Variable	Explanation
T_FC_IRT_X	Maximum temperature reading from the rectangle enclosing the frontal face region.
T_FO_IRT_X	Temperature reading from the spot in the forehead.
T_MO_IRT_X	Maximum temperature reading from the rectangle enclosing the mouth region.
T_CR_IRT_X	Maximum temperature reading from the circle enclosing the right canthus region.
T_CL_IRT_X	Maximum temperature reading from the circle enclosing the left canthus region.
T_CM_IRT_X	Maximum of T_CR_IRT_X and T_CL_IRT_X.

T: Temperature, IRT: Infrared thermography, FC: Frontal face region, FO: Forehead region, MO: Mouth region, CR: Canthus right region, CL: Canthus left region, CM: Maximum of right and left canthus regions

**Table 2. The variables and corresponding definitions of sagittal thermal image reading areas (suffix\_X represents the first and the second captured thermal image, by the number 1 or 2)**

Variable	Explanation
T_FSR_IRT_X	Maximum temperature reading from the rectangle enclosing the right sagittal face region.
T_FSL_IRT_X	Maximum temperature reading from the rectangle enclosing the left sagittal face region.
T_ER_IRT_X	Maximum temperature reading from the rectangle enclosing the right ear region.
T_EL_IRT_X	Maximum temperature reading from the circle enclosing the left ear region.

T: Temperature, IRT: Infrared thermography, FSR: Right sagittal face region, FSL: Left sagittal face region, ER: Right ear, EL: Left ear

## Statistical Analysis

### Measurement Accuracy Assessment Metrics

In order to compare the measurements obtained from either NCIT or IRT devices to assess their body temperature measurement accuracy, we have used the following metrics: the Pearson correlation coefficient, the clinical bias, the SD of the bias samples and the root-mean-square (RMS) difference.

The Pearson correlation coefficient (r-value) is the most common way of measuring a linear correlation. It is a number between -1.0 and 1.0 that measures the strength and direction of the relationship between two sets of data. It is the ratio

between the covariance of two variables and the product of their SDs, so it is essentially a normalized measurement of the covariance.

Basically, the clinical bias between variables a and b is obtained by  $\frac{1}{N} \sum (a - b)$  where N is the number of samples. For simplicity, we depicted the mean and the SD of bias samples by  $\mu_a$  and  $\sigma_a$  respectively. These metrics are defined in standards (28,29). The RMS value of two variables is obtained by  $(\frac{1}{N} \sum (a - b)^2)^{(1/2)}$  where N represents the number of samples.

### Regression Methods to Predict Body Temperatures

In this study, we wanted to reveal if we could approximate NCIT body temperatures by applying a regression analysis to other variables. We wanted to measure how well we could model the relationship between following variable pairs (independent input vs predicted output):

1. T\_FO\_NCIT vs T\_TY\_NCIT.
2. Facial IRT variables vs T\_FO\_NCIT.
3. Sagittal IRT variables vs T\_TY\_NCIT.

In order to determine the regression function to approximate the target samples, the data samples were divided into random training and test sets in proportions of 70% and 30%, respectively. With the training samples, the regression functions that best performed the prediction were determined, and the performances were calculated on the test set. For simplicity, we depicted the predicted samples with the superscript character \* on the target variable. For example, the regression of T\_TY\_NCIT on T\_FSR\_IRT means that T\_FSR\_IRT is the independent input variable to which a regression function is applied and T\_TY\_NCIT\* is the predicted T\_TY\_NCIT samples.

## RESULTS

### Comparison of Forehead and Tympanic NCIT Measurements

The mean and SD pairs of tympanic and forehead NCIT measurements are (36.64, 0.20) and (35.94, 0.39) respectively. In addition, the r-value between them is calculated as 0.31. The bias statistics,  $\mu_d$ ,  $\sigma_d$  and RMS values are (-0.69, 0.38) and 0.79 respectively. The density curves and Bland-Altman plot of the tympanic and forehead NCIT measurements are presented in Figure 2a, 2b. It is observed that with increasing mean temperature values,

the difference between forehead and tympanic NCIT measurements tends to decrease.

The box plots of the NCIT measurements are presented in (Figure 3). It is observed that:

1. Tympanic NCIT measurements are higher than all other parameters with the lowest temperature variance,
2. Forehead NCIT measurements are significantly lower than tympanic NCIT measurements.

### Analysis of Frontal IRT Measurements

The box plots of the first and the second (delayed) frontal IRT measurements are presented in (Figure 3). Looking at these box plots, it is observed that:

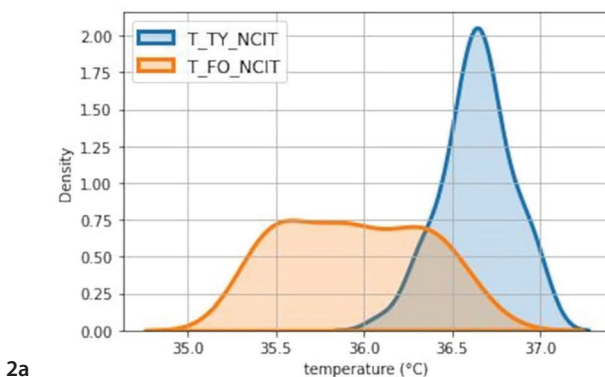
1. The forehead IRT values are lower than the rest of their frontal IRT measurements.
2. The forehead IRT temperatures have the highest SD.
3. The second frontal IRT measurements are lower than the first.

The temperature drop of the second measurements can be interpreted as a result of medical mask removal. Note that, most of the values were decreased after the medical masks were removed.

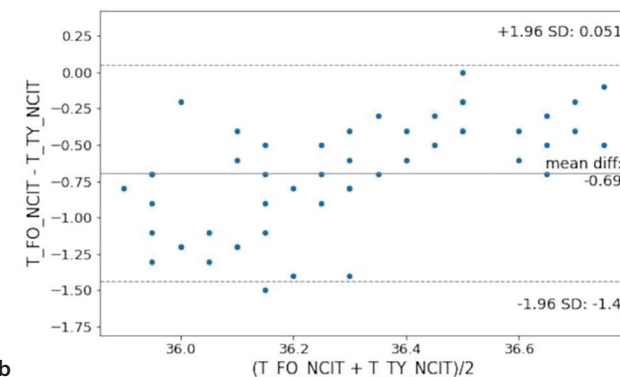
### Analysis of Sagittal IRT Measurements

Box plots for the sagittal thermal camera readings are presented in (Figure 4). In the first two box plots (red colored), NCIT measurements are presented in order to provide comparison. Looking at the box plots, it is observed that:

1. The tympanic NCIT measurements are higher than all other parameters with the lowest temperature variance.
2. The forehead NCIT measurement distribution is more similar to sagittal IRT measurements than to sagittal NCIT.



2a



2b

**Figure 2.** Forehead and tympanic NCIT measurement comparison (a, b). Forehead and tympanic NCIT measurement density curves (a), Bland-Altman plot of forehead and tympanic NCIT measurements, i.e., means vs differences (b)

T: Temperature, TY: Tympanic region, FO: Forehead region, NCIT: Non-contact infrared thermometer, SD: Standard deviation

It is noted that the r-values between the sagittal face and the ear readings [i.e., T\_FSR\_IRT vs T\_right ear (ER)\_IRT and T\_left sagittal face region (FSL)\_IRT vs T\_left ear (EL)\_IRT] are very high. With the exception of two pairs, all the right and left ear measurement samples remain within the limits of agreement.

#### Correlations of Frontal vs Sagittal IRT Measurements

It is found that each sagittal IRT parameter has maximum correlation with one of the second canthus IRT measurements. By comparing these, it can be stated that the r-values increased with the second frontal thermal images. This increase can be interpreted as a result of the removal of medical masks. In both comparisons, the maximum temperatures the left sagittal face have a higher correlation with other frontal sites.

#### Analysis of NCIT vs IRT Measurements

It is observed that the correlation between forehead NCIT and forehead IRT measurements (i.e., T\_FO\_NCIT vs T\_FO\_IRT) are relatively lower than the r-values for the other variables. Overall, the minimum bias SD is 0.61 °C, therefore, the forehead NCIT and the frontal IRT values do not have clinical agreement.

Similarly, the minimum  $\sigma_A$  between tympanic NCIT and sagittal IRT measurements is 0.50 °C, therefore, the tympanic NCIT and the frontal IRT values do not have clinical agreement. It is also observed that the correlation between tympanic NCIT and sagittal IRT measurements is relatively higher than that of forehead NCIT.

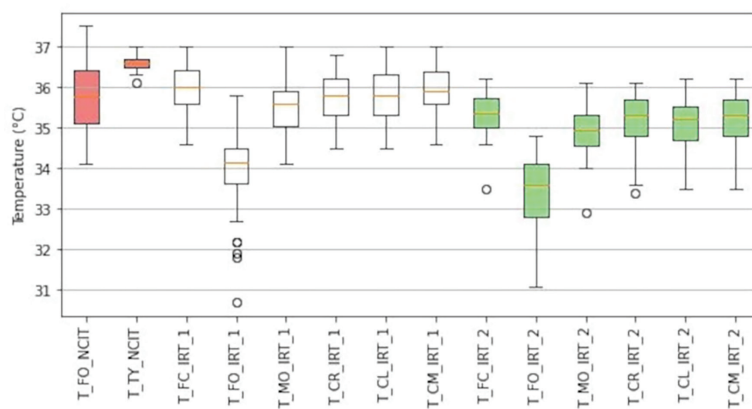


**Figure 3.** Box plots for NCIT and frontal thermal camera readings. NCIT measurements are presented in red color, the first frontal readings are presented in white and the second (delayed) frontal readings are presented in green color

NCIT: Non-contact infrared thermometer, IRT: Infrared thermography, T: Temperature, TY: Tympanic region, FC: Frontal face region, FO: Forehead region, MO: Mouth region, CR: Canthus right region, CL: Canthus left region, CM: Maximum of right and left canthus regions

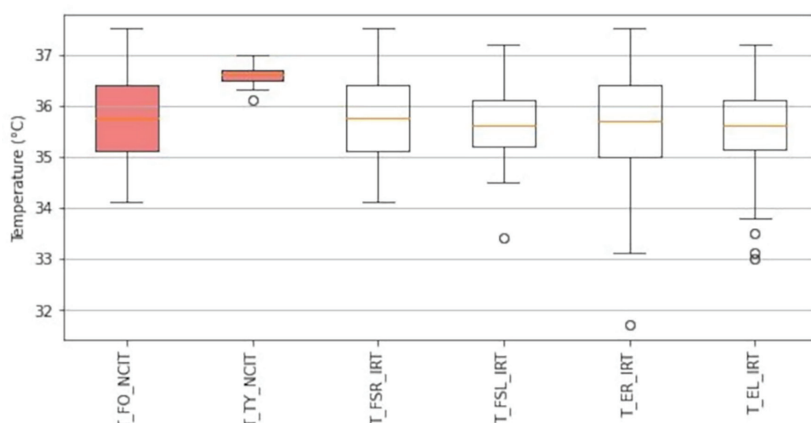


**Figure 4.** Box plots for NCIT and sagittal thermal camera measurements. NCIT measurements are presented in red color

NCIT: Non-contact infrared thermometer, T: Temperature, FO: Forehead region, TY: Tympanic region, FSR: Right sagittal face region, FSL: Left sagittal face region, ER: Right ear, EL: Left ear

## Regression Analysis Results

In this section, the regression analysis results of each NCIT variable on each one of the IRT variables and the analysis of each NCIT variable on another NCIT variable are explained. As a result of this study, we concluded that the first, second and third-order polynomial regression results were very close to each other. This implies that the relationship between these variables are approximately linear. For simplicity, we only presented linear regression solutions.

### Regression of Tympanic NCIT on Forehead NCIT

The linear regression function to model the relationship between forehead and tympanic NCIT samples was determined by the line equation (in °C units):

$$T_{TY\_NCIT}^* = 0.13 * T_{FO\_NCIT} + 32.01 \quad (1)$$

The resultant prediction bias statistics is calculated as (0.04, 0.18).

### Regression of NCIT Temperatures on Frontal IRT

In frontal and sagittal sections, each IRT variable was selected as an independent variable against the corresponding NCIT measurements in that plane and corresponding regression functions were calculated. It is important to note that the

bias statistics and the RMS values for  $T_{TY\_NCIT}$  predictions are lower than those of the  $T_{FO\_NCIT}$ . This means that we can predict tympanic NCIT measurements from frontal IRT measurements with satisfactory agreement, despite the limitations in predicting frontal NCITs from frontal IRTs.

### Regression of Tympanic NCIT on Sagittal IRT

The scatter plot and resultant regression line converting the input variable  $T_{FSR\_IRT}$  to the predicted variable  $T_{TY\_NCIT}^*$  is depicted in (Figure 5). This scatter plot and regression line are shown as an example: other regression line results relating to other variables are not presented to make this article easier to read.

The resultant clinical accuracy metrics to model the relationship between the sagittal IRT variables and  $T_{TY\_NCIT}^*$  are presented in (Table 3). The results indicate that there are significant clinical accuracy and agreement between NCIT measurements. This means that we can predict tympanic NCITs from sagittal IRT measurements (by using separate linear conversion functions for each) and can use them in clinical practice interchangeably.

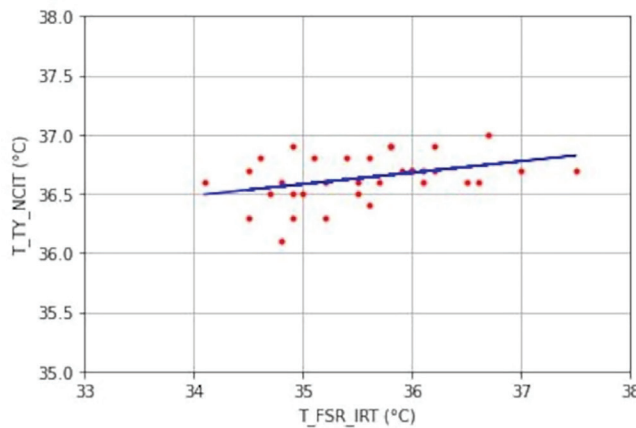


Figure 5. Regression line of tympanic NCIT measurements on sagittal right face IRT measurements

NCIT: Non-contact infrared thermometer, IRT: Infrared thermography, T: Temperature, TY: Tympanic region, FSR: Right sagittal face region

Table 3. The regression error list for each sagittal IRT input variable, to predict tympanic NCIT samples (i.e.,  $T_{TY\_NCIT}^*$ )

	$T_{FSR\_IRT}$	$T_{FSL\_IRT}$	$T_{ER\_IRT}$	$T_{EL\_IRT}$
$\mu_{\Delta}$	0.07	0.06	0.04	0.05
$\sigma_{\Delta}$	0.18	0.18	0.19	0.19
RMS	0.19	0.19	0.19	0.20

T: Temperature, TY: Tympanic region, NCIT: Non-contact infrared thermometer, IRT: Infrared thermography, FSR: Right sagittal face region, FSL: Left sagittal face region, ER: Right ear, EL: Left ear, RMS: Root-mean-square

## DISCUSSION

Using the information gathered in our clinical study, we evaluated the clinical accuracy of the IRTs with respect to reference forehead and tympanic NCITs. The measurements obtained from different NCITs are also compared to each other to assess the degree of agreement. Finally, the linear regression functions were determined to estimate approximate body temperatures from the IRT skin temperatures.

### Clinical Study Limitations

The study group has a mean age of 66.72, despite having the younger samples this is an elderly figure. The age interval may affect the IRT measurements (30). In the future, an extended clinical study including a more balanced population of various age groups may also be conducted.

In this study, the first thermal images were captured 30 seconds after the medical masks were removed. After 60 seconds following the first thermal images, the second images were captured. This sequence was designed to quantify the thermal effect caused by taking off medical masks. It may be considered to continue with a third frontal IRT capture after some delay to minimize any adverse effects of the medical masks.

### Comparison of Forehead NCIT with Tympanic NCIT

It is observed that the forehead and tympanic NCIT measurements have high differences. The mean and SD of tympanic and forehead NCIT measurements are (36.64 °C, 0.20 °C) and (35.94 °C, 0.39 °C) respectively. The reason why tympanic NCIT measurements have a lower SD, might be that the tympanic temperature was found to be the most consistent regardless of the environmental temperature (13,14,15,19).. Besides, each forehead measurement is lower than the corresponding tympanic sample. This result agrees with the results obtained in (19,21,22). In addition, there is another study resulting with a fixed offset between forehead and tympanic NCITs (19) which contradicts our results.

These differences imply that, without any manipulation, our two NCIT devices are not consistent with real body temperatures. This result may be caused by the fact that skin temperature at different sites tends to be sensitive to environmental factors (31). It is also common for various NCIT thermometers display inconsistent measurements (15).

### IRT Analysis in Frontal Face

In the frontal face, it is determined that the maximum facial temperature is strongly correlated with canthus and mouth region IRT measurements, in that order. This finding is similar to previous studies (22,23).

We also revealed that the forehead IRT values are lower than and less correlated with the rest of their frontal IRT samples. These results are consistent with (22,27,31) and may be caused by the fact that the skin temperature at the forehead site tends to be sensitive to environmental factors.

### IRT Analysis in Sagittal Face

In the sagittal face, the hottest point is almost always spotted in the ear region, on both the right and left sides. The right and the left ear IRT temperatures are highly correlated ( $r=0.72$ ). Although the bias mean is being very low ( $\mu_d = -0.09$  °C),  $\sigma_d$  value is 0.53 °C and RMS value is 0.55 °C. Therefore, they cannot be used in clinical practice.

### Effects on IRT After Putting off Medical Mask

The dynamics of thermal inhomogeneities induced by increased concentrations of carbon dioxide in the exhaled air was captured (32). We thought that these inhomogeneities would also affect our frontal IRT measurements.

We observed that the mean value of all frontal IRT measurements at a specific site decreased by the time after the medical mask was removed. The SD values stay almost at the same level. As an example, the mean of the maximum of both canthus IRT temperature values decreases by 0.63 °C and the SD changes only around -0.01 °C. We considered that these temperature changes were caused by the disappearance of the negative effects by time and reaching local thermal stability after the removal of the masks.

### Regression

The corresponding NCIT and IRT measurements in our study are inconsistent regarding clinical accuracy (6,7,22,23,26). This concluded that IRT sensors are more feasible than invasive sensors but should not be the same as those used for measuring core body temperatures (25).

To achieve consistent measurements as in conversion studies, we determined the regression functions to model the relationship between dependent and independent variables (2,22) and after the conversion, we re-evaluated the clinical accuracy. Limpabandhu et al. (26) performed a similar study to ours, which includes capturing IR images in the temple plane. They recorded core body temperatures by using a contact forehead temperature monitoring system and determined that accurate core body temperature prediction could be provided using the linear regression model.

### Regression of Tympanic NCIT on Forehead NCIT

While the majority of studies analyze IRT temperatures against those obtained by thermometers, there are also studies that analyze NCIT values comparatively (15,26). In addition to IRT

vs NCIT comparisons, we also compared forehead against tympanic NCIT measurements. Assuming that each output of these devices is a function of actual core body temperature, we predicted that the fundamental relationship between them could be determined.

We found out that there is a divergence between forehead and tympanic NCIT measurements. The linear regression (1) converts forehead NCIT measurements to tympanic NCIT estimates and produces quite accurate clinical measurements. The resultant bias statistics are (0.04 °C, 0.18 °C) and RMS is 0.19 °C. The forehead temperature becomes an estimate for the tympanic temperature in clinical accuracy after the conversion.

### Regression of NCITs on IRTs

The IRT variables in our dataset have correlations to be considered high to each other, but the bias statistics and RMS values imply that there are major deviations from NCIT references. As a result of this IRT vs NCIT deviation, it is clear that we have to convert the samples from an IRT site to NCIT references, if we want to make a proper body temperature measurement approximation by a thermal camera.

Our regression studies have shown us that when we apply a conversion to sagittal IRT measurements (i.e., ear region), the most accurate tympanic NCIT measurement predictions can be provided. Similarly, Limpabandhu et al. (26) found out that the temple and nose regions were identified as optimal IRT inputs as long as contact forehead thermometer measurements were set as reference.

Naturally, the regression performances of frontal NCIT on frontal IRTs and the regression of tympanic NCIT on frontal IRTs were different. Frontal IRT to tympanic NCIT conversion resulted in better bias statistics and RMS. It produced the outputs that were much more within the acceptable limit. It has a minimum bias mean of 0.04 °C (SD 0.22 °C) and 0.22 °C RMS.

Wang et al. (22) have tried various regression techniques to impute clinical oral temperatures from several frontal IRT sites. Their selected promising results are much better than our regression results. The major reason for this is considered to be the higher variance and different density curve of our forehead thermometer measurements, as shown in (Figure 2a).

Sun et al. (2) calculated the linear regression function of axillary NCIT temperature on IRT facial skin temperature as  $y=0.43 x + 22.57$ , whereas we calculated the conversion of forehead NCIT on facial IRT as  $y=0.08 x + 32.88$ . These two regression functions are quite dissimilar to each other. The main reason may be the use of different NCIT measurement

sites, i.e., axilla vs forehead. Also, thermal cameras and thermometers used in both studies were different. These results emphasized that each experiment should recalculate its own conversion (calibration) functions with regard to the devices, subject types, measurement sites, environment setup etc.

The regression of tympanic NCIT on sagittal IRTs gave slightly better results. It has the bias; 0.04 °C (SD 0.19 °C) and 0.20 °C RMS. The results of these regression methods showed us that one can accurately estimate the body temperature (obtained from the ear channel) from either frontal or sagittal sites on the thermal images.

The standard E1965-98:2016 document defines the maximum permissible errors;  $\pm 0.3$  °C for skin IR thermometers and  $\pm 0.2$  °C in the 36.0-39.0 °C range for ear canal IR thermometers (28). Assuming we had NCIT devices compatible with the standards, the converted NCIT values seem to go out of acceptable accuracy intervals. However, since IEC 80601-2-59: 2017 standard defines the maximum permissible errors;  $\pm 0.5$  °C (in 34.0-39.0 °C range) for IRTs, the converted samples conform to this IRT standard (10).

### CONCLUSION

In this study, a very low agreement was found between forehead and tympanic NCIT measurements. This may be due to the fact that the forehead area is more affected by environmental conditions, whereas the ear canal is relatively closed to external influences. When the IRT measurements were compared with each other, high correlations were determined.

It was also experienced that wearing a medical mask affected the IRT measurements, resulting in an overall increase. This result supports the condition that subjects should be kept waiting for a period of time after they were allowed to take off their masks. As a result, it is thought that it would be more accurate to make IRT measurements in the sagittal plane in cases where the negative effects of the medical mask are likely to be seen.

No clinical agreement was found between IRT and NCIT measurements. It was found that conversion should be performed to estimate body temperature. The clinical agreement was obtained when we estimated the NCIT values by linear regression using the input IRT measurements. The clinical agreement was slightly higher for sagittal plane measurements.

As a result, we showed that real body temperature can be accurately estimated from sagittal face thermal images, especially from the rectangular region surrounding the human ear. The fact that the ear area is more protected from

environmental conditions and does not have obstacles such as medical masks, hats and glasses, means that it should be used in manual use or in fully automated systems. In addition, it may be necessary to capture images with an installation in accordance with the standards and to calculate the conversion functions again for each device and environmental condition.

#### Ethics

**Ethics Committee Approval:** The clinical research, which was a part of the project "Development of Artificial Intelligence-supported Software that Remotely Evaluates Human Body Temperature and Performs High Accuracy Measurements with Thermal Cameras", was approved by İzmir Tinaztepe University Health Sciences Scientific Research and Publication Ethics Committee (protocol code: TUBAYEK: 002, date: 10.03.2021).

**Informed Consent:** Written informed consent was obtained from all subjects.

#### Acknowledgements

The authors gratefully acknowledge İzmir Tinaztepe University Galen Medical Hospital for their outstanding collaboration with the research team during the clinical study.

#### Footnotes

##### Authorship Contributions

Surgical and Medical Practises: E.V., Concept: D.Ö., E.V., Design: D.Ö., E.V., Data Collection or Processing: D.Ö., E.V., Analysis or Interpretation: D.Ö., E.V., Literature Search: D.Ö., E.V., Writing: D.Ö.

**Conflict of Interest:** The authors declare that they have no conflict of interest.

**Financial Disclosure:** This work was supported by Infrared Software Research and Development Consultancy Engineering Ltd. ([www.infraredsoft.com](http://www.infraredsoft.com)), which granted temporary use of a thermal camera and a thermometer for the duration of the study.

#### REFERENCES

1. Werner J. Measurement of temperatures of the human body. *Comprehensive Biomedical Physics*. 2014;5:107-26.
2. Sun G, Matsui T, Kirimoto T, Yao Y, Abe S. Applications of infrared thermography for non-contact and non-invasive mass screening of febrile international travelers at airport quarantine stations. *Application of Infrared to Biomedical Sciences*. 2017;347-58.
3. Nishiura H, Kamiya K. Fever screening during the influenza (H1N1-2009) pandemic at Narita International Airport, Japan. *BMC Infectious Dis*. 2011;11:111.
4. Chiu WT, Lin PW, Chiou HY, Lee WS, Lee CN, Yang YY, et al. Infrared thermography to mass-screen suspected sars patients with fever. *Asia Pac J Public Health*. 2005;17(1):26-8.
5. Ng EY, Kawb G, Chang W. Analysis of IR thermal imager for mass blind fever screening. *Microvasc Res*. 2004;68(2):104-9.
6. Švantner M, Lang V, Skála J, Kohlschütter T, Honner M, Muzika L, et al. Statistical study on human temperature measurement by infrared thermography. *Sensors*. 2022;22(21):8395.
7. Adams S, Bucknall T, Kouzani A. An initial study on the agreement of body temperatures measured by infrared cameras and oral thermometry. *Sci Rep*. 2021;11(1):11901.
8. Cho K, Yoon J. Fever screening and detection of febrile arrivals at an international airport in Korea: association among self-reported fever, infrared thermal camera scanning, and tympanic temperature. *Epidemiol Health*. 2014;36:e2014004.
9. Mouchtouri VA, Christoforidou EP, An der Heiden M, Menel Lemos C, Fanos M, Rexroth U, et al. Exit and entry screening practices for infectious diseases among travelers at points of entry: looking for evidence on public health impact. *Int J Environ Res Public Health*. 2019;16(23):4638.
10. IEC 80601-2-59. Medical electrical equipment-part 2-59: Particular requirements for the basic safety and essential performance of screening thermographs for human febrile temperature screening. International Electrotechnical Commission, International Organization for Standardization. Geneva, Switzerland, 2017.
11. ISO/TR 13154. Medical electrical equipment-deployment, implementation and operational guidelines for identifying febrile humans using a screening thermograph. International Organization for Standardization. Geneva, Switzerland, 2017.
12. Bijur P, Shah P, Esses D. Temperature measurement in the adult emergency department: oral, tympanic membrane and temporal artery temperatures versus rectal temperature. *Emerg Med J*. 2016;33(12):843-7.
13. Fong WWS, Yeo SK, Fook-Chong SMC, Phang JK, Sim E. Comparison of temperature readings using infrared thermometers at three different sites: tympanic, forehead and temporal. *Proceedings of Singapore Healthcare*. 2021;30(1):41-3.
14. Goggins KA, Tetzlaff EJ, Young WW, Godwin AA. SARS-CoV-2 workplace temperature screening: seasonal concerns for thermal detection in northern regions. *Appl Ergon*. 2021;98:103576.
15. Mah AJ, Ghazi Zadeh L, Khoshnam Tehrani M, Askari S, Gandjbakhche AH, Shadgan B. Studying the accuracy and function of different thermometry techniques for measuring body temperature. *Biology*. 2021;10(12):1327.
16. Mairiaux P, Sagot JC, Candas V. Oral temperature as an index of core temperature during heat transients. *Eur J Appl Physiol Occup Physiol*. 1983;50(3):331-41.
17. Geneval I, Cuzzo B, Tasaduq F, Waleed J. Normal body temperature: a systematic review. *Open Forum Infect Dis*. 2019;6(4):032.
18. Aw J. The non-contact handheld cutaneous infra-red thermometer for fever screening during the COVID-19 global emergency. *J Hosp Infect*. 2020;104(4):451.
19. Chen HY, Chen A, Chen C. Investigation of the impact of infrared sensors on core body temperature monitoring by comparing measurement sites. *Sensors*. 2020;20(10):2885.
20. Hakan N, Okumuş N, Aydin M, Küçüközkan T, Tuygun N, Zenciroğlu A. The comparison of temporal temperature measurement method by non-contact infrared thermometer with other body temperature measurement methods. *J Dr Behcet Uz Child Hosp*. 2017;7(2):141-6.
21. Ajčević M, Buoite Stella A, Furlanis G, Caruso P, Naccarato M, Accardo A, et al. A novel non-invasive thermometer for continuous core body temperature: comparison with tympanic temperature in an acute stroke clinical setting. *Sensors*. 2022;22(13):4760.
22. Wang Q, Zhou Y, Ghassemi P, McBride D, Casamento JP, Pfeifer TJ. Infrared thermography for measuring elevated body temperature: clinical accuracy, calibration, and evaluation. *Sensors*. 2021;22(1):215.
23. Zhou Y, Ghassemi P, Chen M, McBride D, Casamento JP, Pfeifer TJ, et al. Clinical evaluation of fever-screening thermography: impact of consensus guidelines and facial measurement location. *J Biomed Opt*. 2020;25(9):097002.
24. Lung-Sang C, Giselle TYC, Ian JL, Cyrus RK. Screening for fever by remote-sensing infrared thermographic camera. *J Travel Med*. 2004;11(5):273-9.

25. Muniz PR, Simão J, Nunes RB, Campos HLM, Santos NQ, Ninke A, et al. Temperature thresholds and screening of febrile people by non-contact measurement of the face using infrared thermography-a methodology proposal. *Sens Biosensing Res.* 2022;37:100513.
26. Limpabandhu C, Hooper F, Li R, Tse Z. Regression model for predicting core body temperature in infrared thermal mass screening. *IPEM Transl.* 2022;3:100006.
27. Putrino A, Raso M, Caputo M, Calace V, Barbato E, Galluccio G. Thermographic control of pediatric dental patients during the SARS-CoV-2 pandemics using smartphones. *Pesquisa Brasileira em Odontopediatria e Clínica Integrada* 2021;21(8).
28. ASTM E1965-98: Standard specification for infrared thermometers for intermittent determination of patient temperature. ASTM Committee E20 on Temperature Measurement. West Conshohocken, PA, USA. 2016:19428.
29. ISO 80601-2-56: Medical electrical equipment-part 2-56: particular requirements for basic safety and essential performance of clinical thermometers for body temperature measurement. International Organization for Standardization: Geneva, Switzerland, 2017.
30. Cheung BM, Chan LS, Lauder IJ, Kumana CR. Detection of body temperature with infrared thermography: accuracy in detection of fever. *Hong Kong Med J.* 2012;18(Suppl 3):31-4.
31. Liu CC, Chang, RE, Chang WC. Limitations of forehead infrared body temperature detection for fever screening for severe acute respiratory syndrome. *Infect Control Hosp Epidemiol.* 2004;25(12):1109-11.
32. Koroteeva E, Shagiyanova A. Infrared-based visualization of exhalation flows while wearing protective face masks. *Phys Fluids* (1994). 2022;34(1):011705.